



Original Paper

Study on prediction of annular trap pressure in ultra-high temperature and high pressure gas wells

Bo-Yuan Yang^{a,b}, Hui Zhang^{a,b,*}, Bao-Kang Wu^b, Kun-Hong Lv^b, Rui Yuan^c,
Yu-Ting Zhou^b, Xing-Yu Li^b, Ze Yang^b

^a Hainan Institute of China University of Petroleum (Beijing), Sanya, 572000, Hainan, China

^b College of Petroleum Engineering, China University of Petroleum-Beijing, Beijing, 102249, China

^c PetroChina Tarim Branch, Korla, 842209, Xinjiang, China



ARTICLE INFO

Article history:

Received 27 February 2025

Received in revised form

3 December 2025

Accepted 3 December 2025

Available online 15 December 2025

Edited by Jia-Jia Fei

Keywords:

Ultra-high temperature and high-pressure wells

Multi-annular pressure prediction

Gas-liquid two-phase coupling

Double packer annulus

ABSTRACT

Accurate calculation of annular trap pressure in ultra-high-temperature and high-pressure (UHTHP) wells is crucial for ensuring the safety and integrity of tubular systems. Existing annular pressure prediction models often fall short due to inadequate consideration of key factors, resulting in reduced accuracy and, consequently, unreliable predictions for tubular safety assessments. This paper examines the underlying mechanisms of annular trap pressure in UHTHP wells and proposes a multi-annular pressure prediction model grounded in the compatibility principle. A gas-liquid two-phase multi-annular pressure coupling model is also developed, incorporating nitrogen injection into the A annulus and utilizing the BWSR equation of state to enhance the model's accuracy. Additionally, a pressure prediction model for the annular space between dual packers is introduced, building upon the multi-annular pressure prediction framework. The results demonstrate that the proposed multi-annular pressure model significantly improves the accuracy of APB predictions for UHTHP gas wells. The findings provide valuable theoretical insights and practical guidance, facilitating more precise prediction of annular trap pressure in extreme downhole conditions and offering essential support for safe operations in these challenging environments.

© 2025 The Authors. Publishing services by Elsevier B.V. on behalf of KeAi Communications Co. Ltd. This is an open access article under the CC BY license (<http://creativecommons.org/licenses/by/4.0/>).

1. Introduction

As the global demand for oil and gas resources continues to rise, an increasing number of ultra-high-temperature and high-pressure (UHTHP) gas wells are being brought into production. These wells operate under more complex conditions, making the prediction of annular trap pressure critical for ensuring wellbore stability, optimizing extraction efficiency, and minimizing operational risks. Annular pressure variation is influenced not only by environmental factors such as temperature and pressure but also by the interactions between liquids and gases within the wellbore, the mechanical behavior of the tubular system, and the thermo-physical properties of the liquids. Therefore, accurately predicting

annular trap pressure is essential for the effective design and safe operation of HP/HT gas wells.

Traditional models for predicting annular trap pressure have several limitations. Single-annulus models often overlook the dynamic interactions between multiple annuli, resulting in inaccurate pressure predictions under complex well conditions. Non-coupled models fail to account for the thermo-hydraulic-mechanical (THM) coupling effects, which are particularly significant in ultra-high-temperature and high-pressure (HPHT) wells, where thermal expansion, liquid compressibility, and phase changes play a crucial role in annular pressure evolution. In contrast, our proposed model introduces a fully coupled multi-annulus pressure prediction framework that incorporates detailed thermodynamic properties of gas-liquid mixtures, accounts for liquid compressibility, and simulates THM interactions across concentric annuli. This approach improves predictive accuracy and expands the model's applicability to deep HPHT wells.

* Corresponding author.

E-mail address: zhanghui9082024@163.com (H. Zhang).

Peer review under the responsibility of China University of Petroleum (Beijing).

In previous studies, researchers have extensively investigated the prediction of annular trap pressure. Early research primarily focused on annular pressure models under conventional temperature and pressure conditions, where simplified models were developed by analyzing the single-phase behavior of liquids and gases in response to temperature and pressure variations. To address the increase in annular pressure and its impact on casing thermal stress, Adams and Maceachran (1994) established an estimation method, while Halal and Mitchell (1994) developed a numerical model for analyzing liquid density and volume changes using the P-V-T equation, and Gao (2002) employed a matrix algorithm to account for casing deformation in both the sealed and free sections of the tubing, establishing a model for predicting annulus closure pressure. Oudeman and Kerem (2006) developed an annular trap pressure prediction model, highlighting the impact of liquid temperature, annular volume, and liquid quality, while Deng et al. (2006) enhanced the accuracy of the model by applying an iterative method for more systematic and precise calculations. Yang et al. (2013) established a prediction model for casing annulus pressure increase in deepwater environments. Zhang et al. (2015a, 2015b, 2016, 2018) calculated annular trap pressure based on the volume compatibility principle and analyzed the effects of fluid thermal conductivity, thermal expansion coefficient, compressibility coefficient, temperature, and production time on annular pressure. Dou et al. (2016) developed a multi-annular trap pressure prediction model that incorporates the effects of annular liquid temperature, pressure, and casing elastic deformation on the annular liquid volume. Zhang (2017) improved the annulus closure pressure prediction model by calculating closure pressures for multiple annuli and double packers using well sectioning. Zhang and Wang (2017) investigated the interaction between annular trap pressure and cement sheath and demonstrated that higher annular pressure increases the risk of cement sheath damage. Wu et al. (2018) solved annular pressure using the Newton downhill method based on deepwater wellbore structure and heat-transfer processes. Xu (2019) refitted the isothermal compression and isobaric expansion coefficients to re-establish the annular trap pressure prediction model. Zhang et al. (2021) examined the influence of oil-pipe deformation under temperature and pressure on the closed annulus and predicted annulus closure pressure between double packers. Sun et al. (2020, 2024a, 2024b) and Zhang et al. (2024a, 2024b, 2024c) advanced the understanding of drilling operations by revealing the rock-breaking mechanisms of PDC cutters, liquid-flow dynamics through vibrating screens, gas invasion behavior in fractured reservoirs, and multiphase-flow temperature prediction models. Jing et al. (2025) conducted a safety-risk analysis of well control in wells with sustained annular pressure and highlighted future technological prospects for improving wellbore stability and operational safety.

Although numerous annular trap pressure models have been developed, most are based on simplified assumptions that limit their applicability under ultra-high-temperature and high-pressure (HPHT) conditions. For example, traditional single-annulus models often overlook the dynamic interactions between multiple annuli and assume idealized fluid behavior, which can result in significant inaccuracies in pressure predictions. Non-coupled models typically treat the wellbore and formation as separate systems, failing to capture the complex thermo-hydraulic-mechanical (THM) coupling effects, particularly under conditions where thermal expansion, fluid compressibility, and phase changes have a substantial impact on annular pressure evolution. Furthermore, many existing models either oversimplify or completely disregard the influence of gas-liquid two-phase flow

characteristics, leading to discrepancies between model predictions and field observations.

In contrast, our model introduces a fully coupled multi-annulus pressure prediction framework that incorporates detailed thermodynamic properties of gas-liquid mixtures, accounts for fluid compressibility, and simulates thermo-hydraulic-mechanical (THM) interactions across concentric annuli. This comprehensive approach improves predictive accuracy and expands the model's applicability to deep HPHT wells, where traditional models are often insufficient. This study aims to accurately predict annular trap pressure in HP/HT gas wells. A multi-annular pressure prediction model is developed based on the compatibility principle, and a gas-liquid two-phase coupling model for multi-annulus pressure is established using the BWSR equation of state, considering nitrogen injection into the annulus. Additionally, a pressure prediction model for the annular space between dual packers is proposed, built on the multi-annular pressure model. The results of this study provide valuable theoretical insights and practical guidance for advancing future annular pressure prediction technologies.

2. Annulus trap pressure calculation model

2.1. Analysis of the mechanism of annular trap pressure

During gas well production, the tubing and cement form the entire wellbore. When the cement does not return to the surface, an annular space is created between the casing layers. The annular pressure is classified into A, B, and C annuli depending on the casing levels, as shown in Fig. 1.

The annular trap pressure is influenced by three primary factors: temperature, annular volume, and the liquid properties within the annulus. Due to cementing operations, if the cement returns higher than the casing shoe of the previous layer, a sealed space is formed. A reduction in annular liquid volume can result in a decrease in annular trap pressure. Assuming no change in the annular liquid mass, temperature fluctuations of the annular liquid during production can lead to volume changes, which subsequently affect the annular pressure. An increase in pressure

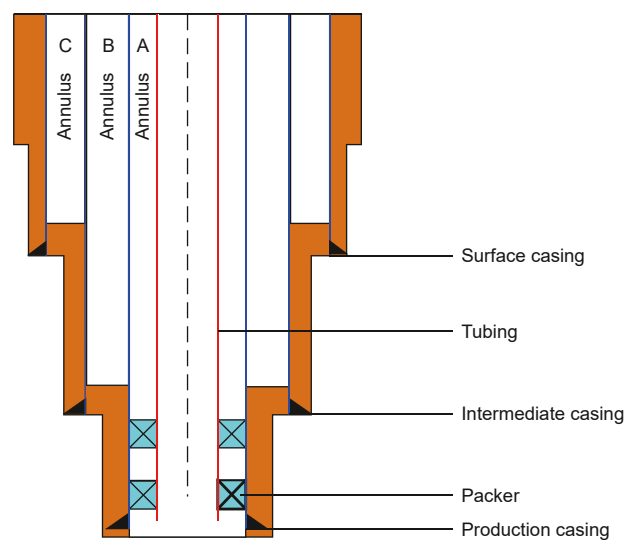


Fig. 1. Schematic diagram of the annulus during the production process of the pipe string.

compresses the liquid, reducing its volume and thereby decreasing the annular trap pressure. Similarly, an increase in casing temperature causes casing expansion, which reduces the annular volume, leading to an increase in annular trap pressure. Although the expansion of the annular volume cannot fully balance the volume expansion of the liquid, it results in an overall increase in annular trap pressure.

Based on the analysis of the mechanism behind the increase in annular trap pressure, the partial differential form of the annular trap pressure increase calculation model (Oudeman and Bacarreza, 1995; Liu et al., 2015) is as follows:

$$\Delta p = \left(\frac{\partial p}{\partial T}\right) \Delta T + \left(\frac{\partial p}{\partial V_{an}}\right) \Delta V_{an} + \left(\frac{\partial p}{\partial m}\right) \Delta m \quad (1)$$

The temperature effect on liquid volume:

$$\alpha_1 = \frac{\Delta V}{V \cdot \Delta T} \quad (2)$$

The pressure effect on liquid volume:

$$K_T = \frac{\Delta V}{V \cdot \Delta P} \quad (3)$$

Annular trap pressure increase formula:

$$\Delta p = \frac{\alpha_1}{K_T} \Delta T - \frac{1}{K_T V_{an}} \Delta V_{an} + \frac{1}{K_T V_1} \Delta V_1 \quad (4)$$

In the formula:

- α_1 —the liquid's thermal expansion coefficient, 1/°C;
- K_T —the liquid's isothermal compressibility coefficient, 1/MPa;
- ΔT —the temperature change of the liquid, °C;
- ΔP —the increase in annular trap pressure, MPa;
- ΔV_{an} —the total change in annular volume, m³;
- ΔV_1 —the change in the volume of the annular liquid, m³.

Assuming that the annular space is sealed, with no inflow or outflow of annular liquid, the entire process of increasing annular trap pressure can be regarded as a combination of two processes: a constant-pressure thermal expansion process due to temperature rise and an isothermal compression process due to pressure change. Therefore, the integral formula for the annular trap pressure increase is given by:

$$\int_T \alpha_1 V_T dT - \int_P K_T V_P dP = \int_{V_1} \frac{1}{V} dV \quad (5)$$

In the formula:

- V_T —the volume of the liquid under constant-pressure thermal expansion, m³;
- V_P —the volume of the liquid under isothermal compression, m³.

2.2. Annular liquid volume calculation model

The annular liquid volume refers to the volume of liquid in the annulus that changes due to variations in temperature and pressure. According to Eq. (5), it is evident that both α_p and K_T are key factors influencing the annular liquid volume. The partial differential calculation formula is given by:

$$\alpha_p = \frac{1}{V} \left. \frac{\partial V}{\partial T} \right|_p = \frac{1}{\nu_m} \left. \frac{\partial \nu_m}{\partial T} \right|_p \quad (6)$$

$$K_T = -\frac{1}{V} \left. \frac{\partial V}{\partial P} \right|_T = -\frac{1}{\nu_m} \left. \frac{\partial \nu_m}{\partial P} \right|_T \quad (7)$$

In the formula:

- α_p —the isobaric expansion coefficient, 1/MPa;
- ν_m —the molar volume of the annular liquid, m³/mol.

In order to more accurately obtain the volume change of the annular liquid due to thermal expansion, the best fitting isothermal compression coefficient and isobaric expansion coefficient (Yin and Gao, 2014) are used, and the calculation formula is:

$$\alpha_p = \frac{a_1 + a_2 T + a_3 T^2 + a_4 T^3 + a_5 P + a_6 P^2}{1 + a_7 T + a_8 P} \quad (8)$$

$$K_T = \frac{b_1 + b_2 T + b_3 T^2 + b_4 P}{1 + b_5 T + b_6 P + b_7 P^2} \quad (9)$$

Due to the significant variation in axial temperature distribution in high-temperature, high-pressure gas wells, previous methods that averaged the temperature changes across the entire annulus to calculate liquid volume changes introduced substantial errors. These methods did not accurately calculate the annular liquid volume and failed to account for the changes in thermo-physical properties caused by temperature and pressure fluctuations. To obtain a more precise estimation of the annular liquid volume, the annulus is discretized into small segments, and the liquid volume change within each segment is calculated. The sum of these individual segment changes gives the total annular liquid volume change. By substituting the fitted Eqs. (8) and (9) into Eq. (5), the final volume change of the annular liquid for each segment can be expressed as:

$$V_1 = e^{(A_2 - A_1) - (D_2 - D_1)} \quad (10)$$

$$\Delta V_1 = e^{(A_2 - A_1) - (D_2 - D_1)} - V_{ini} \quad (11)$$

In the formula:

- V_1 —the annular liquid volume under certain temperature and pressure conditions, m³;
- V_{ini} —the initial annular liquid volume, m³.

Among them, A_1 and A_2 are the integrals of the isobaric expansion coefficient fitting formula:

$$A_1 = \frac{1}{6a_7^4} * \left(\frac{6a_2 T_1 a_7^3 + 3a_3 T_1^2 a_7^3 + 2a_4 T_1^3 a_7^3 - 6a_3 T_1 a_7^2 (1 + a_8 P_1) - 3a_4 *}{T_1^2 a_7^2 (1 + a_8 P_1) + 6a_4 T_1 a_7 (1 + a_8 P_1)^2 - 6 \ln(1 + a_7 T_1 + a_8 P_1) *} \right) \left[a_4 (1 + a_8 P_1)^3 + a_2 a_7^2 (1 + a_8 P_1) - a_3 a_7 (1 + a_8 P_1)^2 \right] \quad (12)$$

$$A_2 = \frac{1}{6a_7^4} * \left(\begin{aligned} &6a_2T_2a_7^3 + 3a_3T_2^2a_7^3 + 2a_4T_2^3a_7^3 - 6a_3T_2a_7^2(1 + a_8P_2) - 3a_4^* \\ &T_2^2a_7^2(1 + a_8P_2) + 6a_4T_2a_7(1 + a_8P_2)^2 - 6 \ln(1 + a_7T_2 + a_8P_2)^* \\ &[a_4(1 + a_8P_2)^3 + a_2a_7^2(1 + a_8P_2) - a_3a_7(1 + a_8P_2)^2] \end{aligned} \right) \quad (13)$$

In the formula:

T_1 —the annulus temperature before production, °C;

T_2 —the annulus temperature during production, °C;

P_1 —the annulus pressure before production, MPa;

P_2 —the annulus pressure during production, MPa.

D_1 and D_2 are the integrals of the isothermal compressibility fitting formula:

$$D_1 = \frac{b_4}{2b_7} \ln \left(P_1^2 + \frac{b_6}{b_7} P_1 + \frac{1+b_5T_2}{b_7} \right) + \frac{2b_7(b_1+b_2T_2+b_3T_2^2) - b_4b_6}{2b_7} * \frac{2}{\sqrt{4(1+b_5T_2)b_7}} * \arctan \left(\frac{2P_1b_7+b_6}{\sqrt{4(1+b_5T_2)b_7}} \right) \quad (14)$$

$$D_2 = \frac{b_4}{2b_7} \ln \left(P_2^2 + \frac{b_6}{b_7} P_2 + \frac{1+b_5T_2}{b_7} \right) + \frac{2b_7(b_1+b_2T_2+b_3T_2^2) - b_4b_6}{2b_7} * \frac{2}{\sqrt{4(1+b_5T_2)b_7}} * \arctan \left(\frac{2P_2b_7+b_6}{\sqrt{4(1+b_5T_2)b_7}} \right) \quad (15)$$

The above formula can be used to calculate the annular liquid volume $V_{1,A}$, $V_{1,B}$, $V_{1,C}$ of A, B, and C under different conditions for A, B, and C. To account for non-Newtonian liquid behavior, we propose modifying the liquid volume calculation models to include rheological properties. The liquid volume change equations (Eqs. (6–14)) will be expanded to incorporate viscosity functions that are dependent on shear rate and other rheological parameters. Additionally, constitutive equations for non-Newtonian fluids, such as the Power-Law model or the Herschel-Bulkley model, will be considered to enhance the model's accuracy in describing viscous or contaminated fluids.

2.3. Annulus volume calculation model

The annular volume refers to the volume of the enclosed space formed by the inner and outer tubing. The variation in annular volume is primarily caused by thermal expansion due to temperature changes, the bulging effect induced by radial compression of the tubing, axial forces causing radial displacement, and radial displacements at the cemented section.

(1) Radial displacement due to temperature variations in the free section of the tubing:

$$u_1 = (1 + 2\mu_T)\alpha_T r \Delta T \quad (16)$$

In the formula:

α_T —the thermal expansion coefficient of the pipe string, $1/^\circ\text{C}$;

μ_T —the Poisson's ratio of the pipe string, dimensionless;

r —the radius of the calculation point of the pipe string, m;

ΔT —the temperature change of the pipe string, °C.

(2) Radial displacement due to annular pressure

When the annular pressure increases, the liquid in the annulus exerts pressure on the outer and inner casings, causing the annular volume to expand. This results in the compression of the outer casing and the bulging of the inner casing, as shown in Fig. 2.

The calculation formula for this effect is given by:

$$u_2 = \frac{1 + \mu_T}{E} \left[\frac{r_i^2 r_o^2 + (1 - 2\mu_T)r_i^2 r^2}{(r_o^2 - r_i^2)r} p_i - \frac{r_i^2 r_o^2 + (1 - 2\mu_T)r_o^2 r^2}{(r_o^2 - r_i^2)r} p_o \right] \quad (17)$$

In the formula:

E —the elastic modulus of the tubing, MPA;

p_i —the internal pressure of the tubing, MPA;

p_o —the external pressure of the tubing, MPA;

r_i —the inner diameter of the tubing, m;

r_o —the outer diameter of the tubing, m.

(3) Radial displacement caused by axial force:

$$u_3 = \mu \alpha \Delta T r - \frac{2\mu^2(r_i^2 \Delta p_i - r_o^2 \Delta p_o)}{E(r_o^2 - r_i^2)} r \quad (18)$$

(4) Radial displacement of sealing section:

$$u_4 = -\frac{r_i(1 + \mu)}{E} \left[(1 - \mu) + \mu \frac{m + 1 - n}{m - 1 + n} \right] \Delta p + (1 + \mu)r_i \alpha \Delta T \quad (19)$$

In the formula:

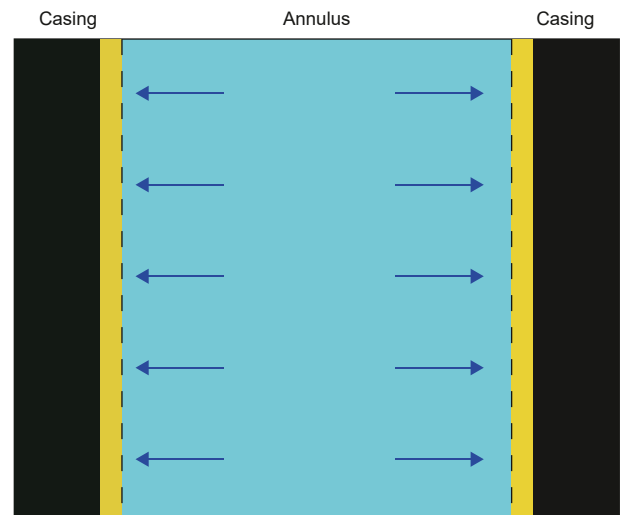


Fig. 2. Diagram of column radial displacement caused by annulus pressure.

$$n = \frac{E(1 + \mu)}{E(1 + \mu')}$$

$$m = [1 + (1 - 2\mu)n] \frac{r_o^2}{r_i^2}$$

μ' —the Poisson's ratio of cement sheath, dimensionless;
 E' —the elastic modulus of cement sheath, MPa;
 r_i —the inner diameter of the casing, m;
 r_o —the outer diameter of the casing, m.

2.4. Multi-annulus trap pressure calculation model

When there are multiple annuli in a production gas well, the mutual influence and coupling between different annuli must be considered.

Annulus volume calculation model of A annulus:

The radial displacement of its outer wall due to temperature change is:

$$u_{A1} = (1 + 2\mu)\alpha_T r_{to} \Delta T \tag{20}$$

The radial displacement caused by the annular pressure on its outer wall is:

$$u_{A2} = -\frac{1 + \mu}{E} \frac{r_{ti}^2 r_{to} + (1 - 2\mu)r_{to}^3}{(r_{to}^2 - r_{ti}^2)} \Delta p_A \tag{21}$$

In the free section, the radial displacement caused by the B annulus on the production casing is:

$$u_{A3} = \frac{1 + \mu}{E} \left[\frac{r_{ci} r_{co}^2 + (1 - 2\mu)r_{ci}^3}{(r_{co}^2 - r_{ci}^2)} \Delta p_A - \frac{r_{ci} r_{co}^2 + (1 - 2\mu)r_{co}^2 r_{ci}}{(r_{co}^2 - r_{ci}^2)} \Delta p_B \right] \tag{22}$$

The axial force on the oil pipe causes the outer wall displacement of the oil pipe to be:

$$u_{A4} = \mu\alpha\Delta T r_{to} + \frac{2\mu^2 r_{to}^2 \Delta p_A}{E(r_{to}^2 - r_{ti}^2)} r_{to} \tag{23}$$

The axial force causes radial displacement of the inner wall of the production casing:

$$u_{A5} = \mu\alpha\Delta T r_{ci} - \frac{2\mu^2 (r_{ci}^2 \Delta p_A - r_{co}^2 \Delta p_B)}{E(r_{co}^2 - r_{ci}^2)} r_{ci} \tag{24}$$

Radial displacement of sealing section:

$$u_{A6} = -\frac{r_i^2(1 + \mu)}{E} \left[(1 - \mu) + \mu \frac{m + 1 - n}{m - 1 + n} \right] \Delta p_A + (1 + \mu)r_i^2 \alpha \Delta T \tag{25}$$

Then the volume change of annulus A is:

$$\Delta V_{A.f} = \pi h_1 \left((r_{ci} + u_{A3} + u_{A5})^2 - (r_{to} + u_{A1} + u_{A2} + u_{A4})^2 - (r_{ci}^2 - r_{to}^2) \right) \tag{26}$$

$$\Delta V_{A.s} = \pi h_2 \left((r_{ci} + u_{A6})^2 - (r_{to} + u_{A1} + u_{A2} + u_{A4})^2 - (r_{ci}^2 - r_{to}^2) \right) \tag{27}$$

$$\Delta V_A = \Delta V_{A.f} + \Delta V_{A.s} \tag{28}$$

When the temperature is T , the volume of annulus A is:

$$V_A = V_{A.f} + V_{A.s} \tag{29}$$

In the formula:

h_1 —the free segment length, m;

h_2 —the length of the sealing section, m;

$\Delta V_{A.f}$ —the change in volume of the free segment of the A-shaped annulus;

$\Delta V_{A.s}$ —the change in annular volume of A-annular sealed section;

$V_{A.f}$ —The volume of the free segment of the A-annulus at temperature T ;

$V_{A.s}$ —the volume of the annulus in the sealed section A at temperature T ;

V_A —the volume of A-annulus at temperature T .

B annulus volume calculation model:

In the free section, the radial displacement of the outer wall of the production casing due to temperature change is:

$$u_{B1} = (1 + 2\mu_T)\alpha_T r_{co} \Delta T_1 \tag{30}$$

In the formula:

ΔT_1 —the changing temperature for production casing, °C.

In the free section, the production casing undergoes radial displacement under the action of internal pressure Δp_A and external pressure Δp_B :

$$u_{B2} = \frac{1 + \mu}{E} \left[\frac{r_{ci}^2 r_{co} + (1 - 2\mu)r_{ci}^2 r_{co}}{(r_{co}^2 - r_{ci}^2)} \Delta p_A - \frac{r_{ci}^2 r_{co} + (1 - 2\mu)r_{co}^3}{(r_{co}^2 - r_{ci}^2)} \Delta p_B \right] \tag{31}$$

In the free section, the technical casing undergoes radial displacement under the action of internal pressure Δp_B and external pressure Δp_C :

$$u_{B3} = \frac{1 + \mu}{E} \left[\frac{r_{ci2} r_{co2}^2 + (1 - 2\mu)r_{ci2}^3}{(r_{co2}^2 - r_{ci2}^2)} \Delta p_B - \frac{r_{ci2}^2 r_{co2}^2 + (1 - 2\mu)r_{co2}^2 r_{ci2}}{(r_{co2}^2 - r_{ci2}^2)} \Delta p_C \right] \tag{32}$$

The radial displacement of the outer wall of the production casing caused by the axial force:

$$u_{B4} = \mu\alpha\Delta T_1 r_{co} - \frac{2\mu^2 (r_{ci}^2 \Delta p_A - r_{co}^2 \Delta p_B)}{E(r_{co}^2 - r_{ci}^2)} r_{co} \tag{33}$$

Radial displacement of the inner wall of the technical casing caused by axial force:

$$u_{B5} = \mu\alpha\Delta T_2 r_{ci2} - \frac{2\mu^2 (r_{ci2}^2 \Delta p_B - r_{co2}^2 \Delta p_C)}{E(r_{co2}^2 - r_{ci2}^2)} r_{ci2} \tag{34}$$

Radial displacement of sealing section:

$$u_{B6} = -\frac{r_{ci2}(1 + \mu)}{E} \left[(1 - \mu) + \mu \frac{m + 1 - n}{m - 1 + n} \right] \Delta p_B + (1 + \mu)r_{ci2}\alpha\Delta T_2 \quad (35)$$

In the formula:

ΔT_2 —the temperature change of the casing, °C.

Then the volume change of annulus B is:

$$\Delta V_{B-f} = \pi h_3 \left((r_{ci2} + u_{B3} + u_{B5})^2 - (r_{co1} + u_{B1} + u_{B2} + u_{B4})^2 - (r_{ci2}^2 - r_{co}^2) \right) \quad (36)$$

$$\Delta V_{B-s} = \pi h_3 \left((r_{ci2} + u_{B6})^2 - (r_{co1} + u_{B1} + u_{B2} + u_{B4})^2 - (r_{ci2}^2 - r_{co}^2) \right) \quad (37)$$

$$\Delta V_B = \Delta V_{B-f} + \Delta V_{B-s} \quad (38)$$

When the temperature is T , the volume of annulus B is:

$$V_B = V_{B-f} + V_{B-s} \quad (39)$$

In the formula:

h_3 —the length of B annulus, m.

ΔV_{B-f} —the change in volume of the free segment of the B-shaped annulus;

ΔV_{B-s} —the change in annular volume of B-annular sealed section;

V_{B-f} —the volume of the free segment of the B-annulus at temperature T ;

V_{B-s} —the volume of the annulus in the sealed section B at temperature T ;

V_B —the volume of B-annulus at temperature T .

C annulus volume calculation model:

The radial displacement of the technical casing affected by temperature is:

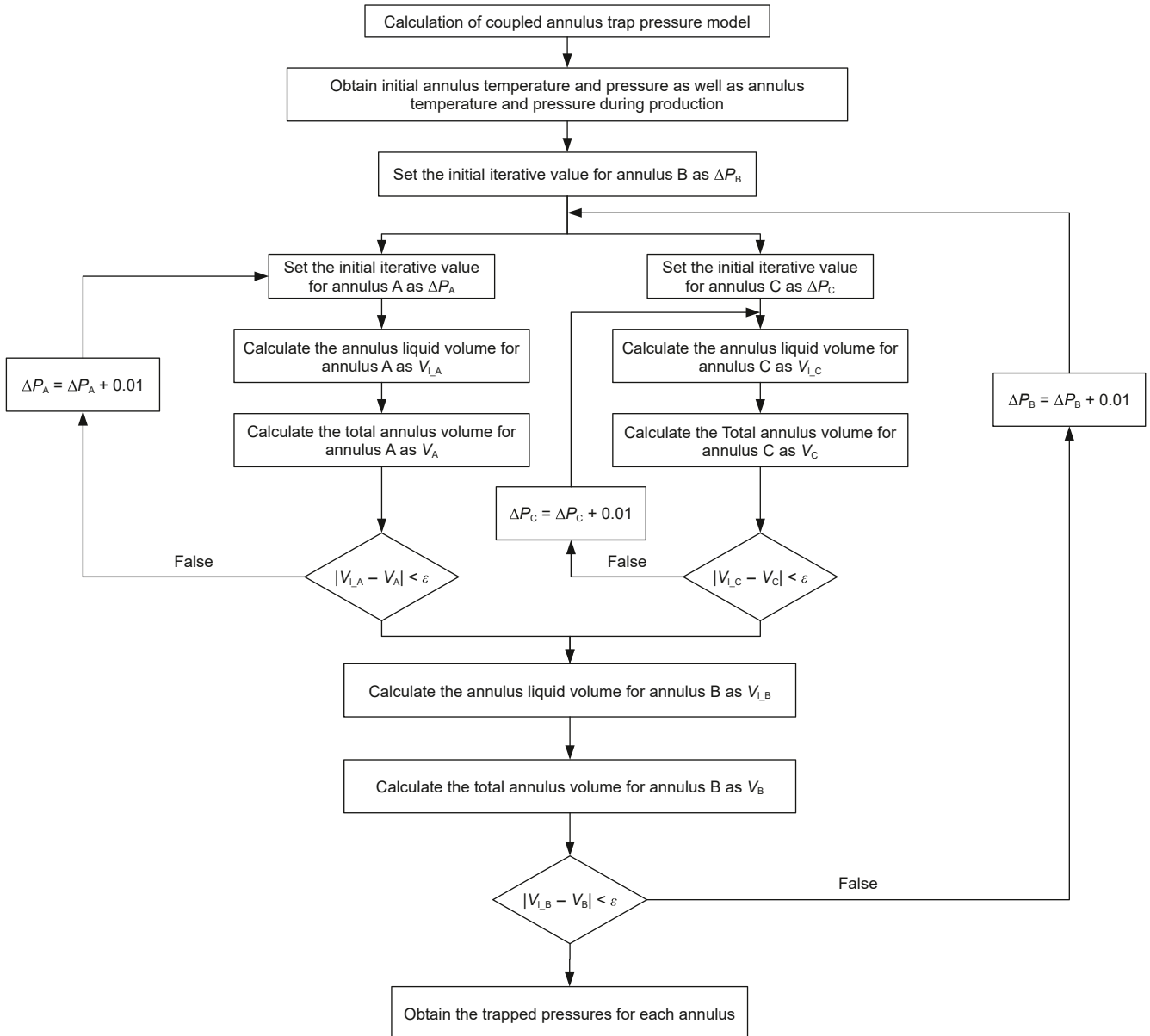


Fig. 3. Multi-annulus pressure calculation flow chart.

$$u_{C1} = (1 + 2\mu_T)\alpha_T r_{co2} \Delta T_2 \tag{40}$$

Radial displacement of technical casing caused by pressure:

$$u_{C2} = \frac{1+\mu}{E} \left[\frac{r_{ci2} r_{co2}^2 + (1-2\mu)r_{ci2}^3 \Delta p_B}{(r_{co2}^2 - r_{ci2}^2)} - \frac{r_{ci2} r_{co2}^2 + (1-2\mu)r_{co2}^2 r_{ci2} \Delta p_C}{(r_{co2}^2 - r_{ci2}^2)} \right] \tag{41}$$

The radial displacement of the outer wall of the technical casing caused by the axial force:

$$u_{C3} = \mu\alpha\Delta T_2 r_{co2} - \frac{2\mu^2(r_{ci2}^2 \Delta p_B - r_{co2}^2 \Delta p_C)}{E(r_{co2}^2 - r_{ci2}^2)} r_{co2} \tag{42}$$

Radial displacement of sealing section:

$$u_{C4} = -\frac{r_{ci3}(1+\mu)}{E} \left[(1-\mu) + \mu \frac{m+1-n}{m-1+n} \right] \Delta p_C + (1+\mu)r_{ci3}\alpha\Delta T_3 \tag{43}$$

In the formula:

ΔT_3 —the temperature change of the surface casing, °C.

Then the volume change of annulus C is:

$$\Delta V_{C.f} = \pi h_4 \left((r_{ci3} + u_{C3} + u_{C5})^2 - (r_{co2} + u_{C1} + u_{C2} + u_{C4})^2 - (r_{ci3}^2 - r_{co2}^2) \right) \tag{44}$$

$$\Delta V_{C.s} = \pi h_4 \left((r_{ci3} + u_{C6})^2 - (r_{co2} + u_{C1} + u_{C2} + u_{C4})^2 - (r_{ci3}^2 - r_{co2}^2) \right) \tag{45}$$

$$\Delta V_C = \pi h_4 \left((r_{ci3} + u_{C4})^2 - (r_{co2} + u_{C1} + u_{C2} + u_{C3})^2 - (r_{ci3}^2 - r_{co2}^2) \right) \tag{46}$$

$$V_C = V_{C.f} + V_{C.s} \tag{47}$$

In the formula:

h_4 —the length of C annulus, m;

$\Delta V_{C.f}$ —the change in volume of the free segment of the C-shaped annulus;

$\Delta V_{C.s}$ —the change in annular volume of C-annulus sealed section;

$V_{C.f}$ —the volume of the free segment of the C-annulus at temperature T ;

$V_{C.s}$ —the volume of the annulus in the sealed section C at temperature T ;

V_C —the volume of C-annulus at temperature T .

The entire annular trap pressure calculation process is shown in Fig. 3:

3. Gas-liquid two-phase annular trap pressure coupling model

When inert gases such as nitrogen are injected into the annulus, a two-phase gas-liquid mixture is formed, resulting in an annular gas column, as shown in Fig. 4. Due to the significantly higher compressibility of the gas compared to the liquid, the volume expansion of the liquid and the changes in annular volume caused by variations in temperature and pressure will affect the physical properties of the gas in the annulus, leading to

compression of the gas. Therefore, on the basis of the existing full-liquid phase annular trap pressure prediction model, the coupling of gas and liquid phases under different temperature and pressure conditions must be considered.

In a single-phase annulus, the main difference between a gas-liquid two-phase model and a pure liquid phase model lies in the coupling of the gas and liquid phases, which must be accounted for in the calculation. The volume of the liquid, influenced by temperature and pressure, compresses the gas, ultimately ensuring that the total volume of the gas and liquid matches the total annular volume. According to the principle of volume compatibility, the annular volume change calculation model can be expressed as:

$$\Delta V_{an} = \Delta V_l + \Delta V_g \tag{48}$$

In the formula:

ΔV_{an} —the change in annulus volume, m³;

ΔV_l —the change in annulus liquid volume, m³;

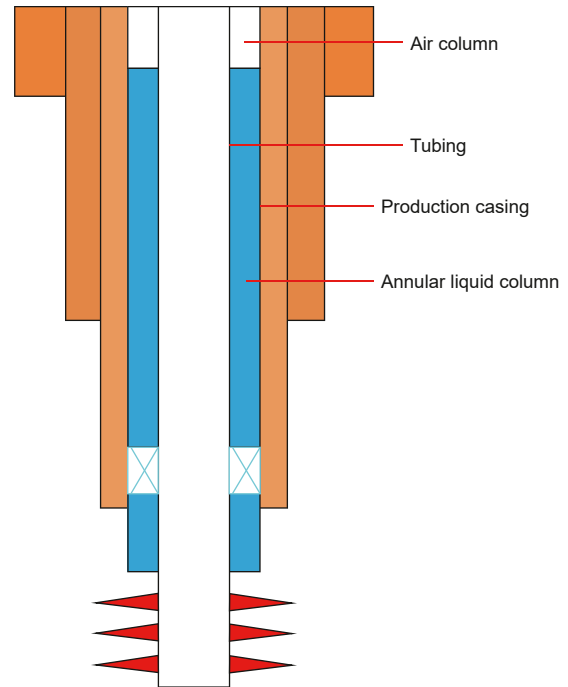


Fig. 4. Diagram of gas-liquid two-phase annulus.

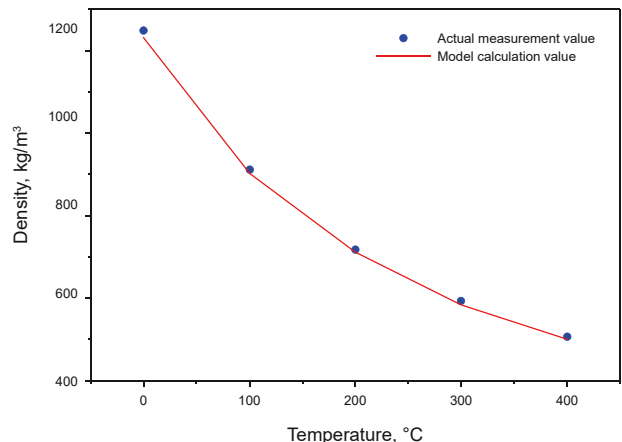


Fig. 5. Comparison between nitrogen model calculation and measured data.

ΔV_g —the change in annulus gas volume, m^3 .

The liquid volume in the annulus can be calculated by Eq. (10) and the annulus volume can be calculated by Eq. (27), so it is necessary to calculate the change in the annulus gas volume.

Compared to the ideal gas law and the Peng-Robinson (PR) equation of state, the Benedict-Webb-Rubin-Starling (BWSR) equation provides significantly improved accuracy in describing the thermodynamic behavior of real gases under high-pressure and high-temperature (HPHT) conditions. The ideal gas law assumes negligible molecular interactions and is only applicable under low-pressure, moderate-temperature regimes, which is inadequate for deep gas wells. The PR equation, although widely used in petroleum engineering for phase equilibrium calculations, tends to underestimate compressibility and density near the critical point or under extreme thermal environments.

In contrast, the BWSR equation incorporates higher-order terms to account for intermolecular forces and volume exclusions, enabling it to more accurately characterize non-ideal behavior of gas-phase mixtures at elevated temperatures and pressures. As a result, the use of the BWSR equation enhances the reliability of pressure and temperature predictions in HPHT

annular systems, particularly when liquid compressibility and real-gas effects are non-negligible.

According to the BWSR state equation, it is changed into a functional form:

$$f(\rho) = \rho RT + \left(B_0 RT - A_0 - \frac{C_0}{T^2} + \frac{D_0}{T^3} + \frac{E_0}{T^4} \right) \rho^2 + \left(bRT - a - \frac{d}{T} \right) \rho^3 + \alpha \left(a + \frac{d}{T} \right) \rho^6 + \frac{c\rho^3}{T^2} (1 + \gamma\rho^2) e^{(-\gamma\rho^2)} - P = 0 \tag{49}$$

The choice of the BWSR state equation for modeling the gas phase is justified by its ability to more accurately characterize non-ideal behavior of gas-phase mixtures at elevated temperatures and pressures compared to the ideal gas law and the PR equation. The ideal gas law assumes negligible molecular interactions and is only applicable under low-pressure, moderate-temperature regimes, which is inadequate for deep gas wells. The PR equation, although widely used in petroleum engineering for phase equilibrium calculations, tends to underestimate compressibility and density near the critical point or under extreme thermal environments. In

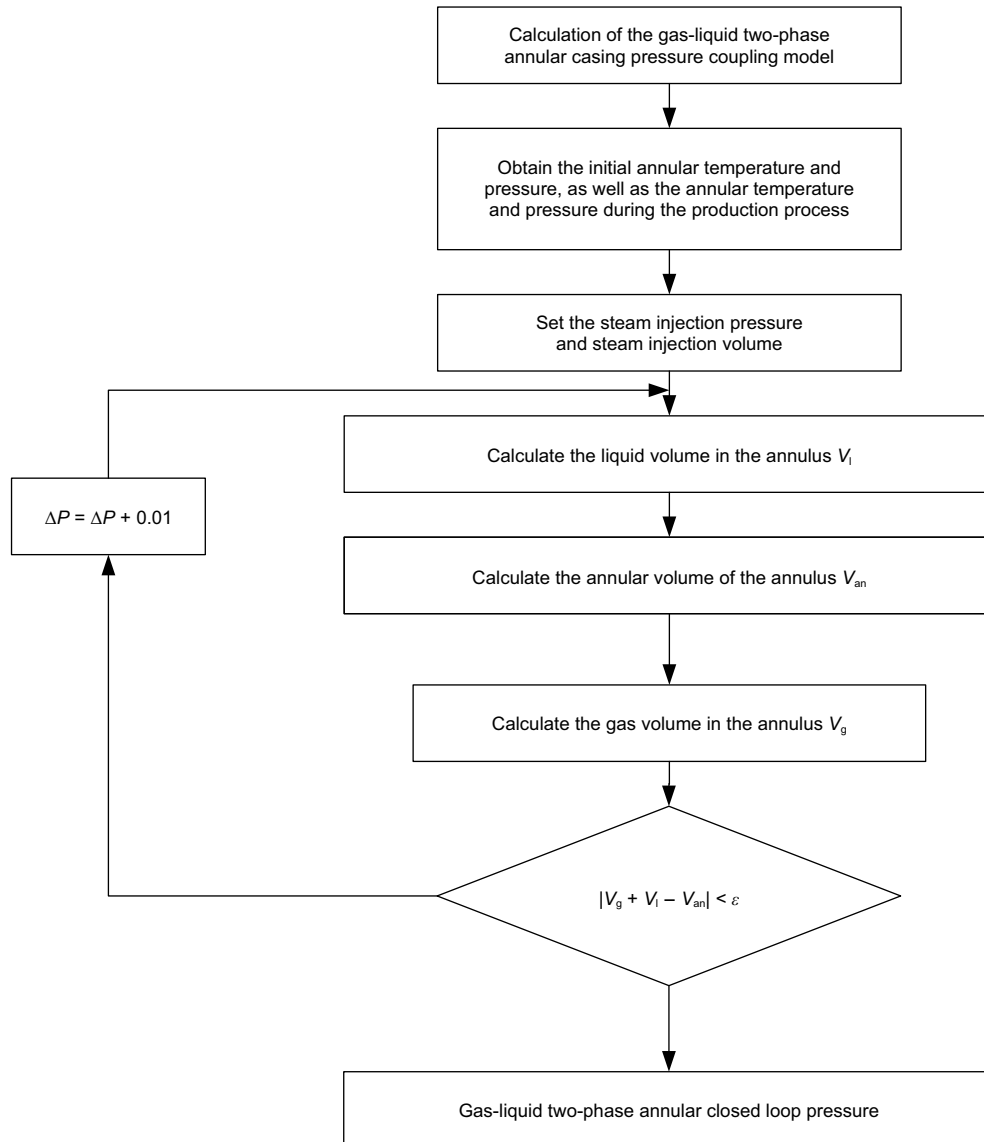


Fig. 6. Flow chart of gas-liquid two-phase annulus pressure calculation.

contrast, the BWSR equation incorporates higher-order terms to account for intermolecular forces and volume exclusions, enabling it to provide improved accuracy in describing the thermodynamic behavior of real gases under HPHT conditions.

The annular gas density is iteratively calculated using the secant method (Wang, 2023):

$$\rho_{k+1} = \frac{\rho_{k-1}f(\rho_k) - \rho_k f(\rho_{k-1})}{f(\rho_k) - f(\rho_{k-1})} \tag{50}$$

The initial value of the iteration is $\rho_1 = 0$; $\rho_2 = P/RT$.

Taking N_2 as an example, the comparison between the model calculated value and the measured value is shown in Fig. 5:

The change of gas volume under the influence of annular trap pressure is:

$$\Delta V_g = V_g - \frac{\rho_1 V_g}{\rho_2} \tag{51}$$

In the formula:

ρ_1 —the initial density of the gas, m^3 ;

ρ_2 —the final density of the gas, m^3 ;

V_g —the initial volume of the gas, m^3 .

The calculation process is shown in Fig. 6:

4. Calculation of annular trap pressure between double packers

The calculation model of the multi-packer annulus closed pressure is consistent with the pure liquid phase closed pressure model containing only the sealing section under the single annulus, as shown in Fig. 7. The annulus between the double packers is referred to as the annulus between the double packers, the annulus A above the production packer is the upper annulus,

and the distance between the double packers is the spacing between the double packers.

The calculation model is:

$$\Delta V_{A-P} = \pi \left((r_{ci} + u_{A6})^2 - (r_{to} + u_{A1} + u_{A2} + u_{A4})^2 - (r_{ci}^2 - r_{to}^2) \right) \Delta h \tag{52}$$

In the formula:

Δh —the double packer spacing, m.

The calculation process of the double packer annulus closure pressure is shown in Fig. 8:

5. Case calculation

In order to verify the accuracy of the model, the annular trap pressure experimental results in the literature were used to verify the accuracy of the model in this paper. The basic parameters of the experiment are shown in Table 1:

According to the experimental basic data and size relationship, the annular trap pressure data of the three annuli A, B, and C under cementing and non-cementing conditions are compared. The results are shown in Figs. 9–11.

To provide a more comprehensive evaluation of the model's prediction accuracy, specific error indicators such as root mean square error (RMSE) and mean absolute percentage error (MAPE) were calculated and presented in Table 2. The results show that the average error between the predicted and experimental data is minimal, indicating the high accuracy and effectiveness of the proposed multi-annular trap pressure prediction model. Comparing the experimental results with the predicted data, the average error is shown in Table 2:

As shown in Figs. 9–11 and Table 2, the annulus closure pressure prediction model established in this paper is highly consistent

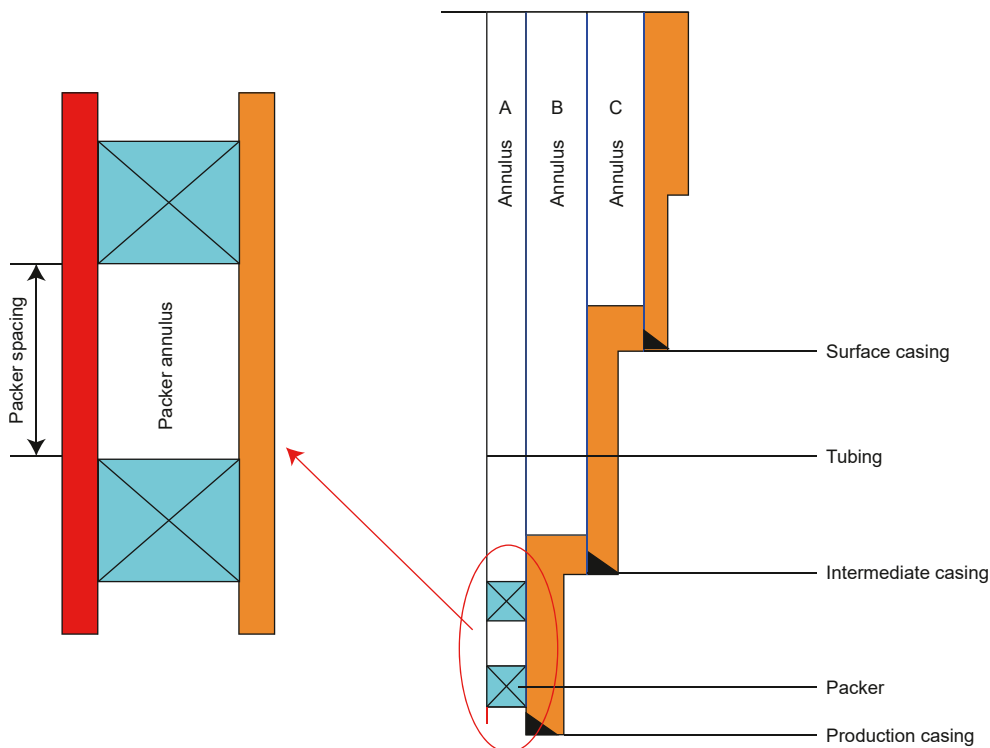


Fig. 7. Annulus diagram of two packers.

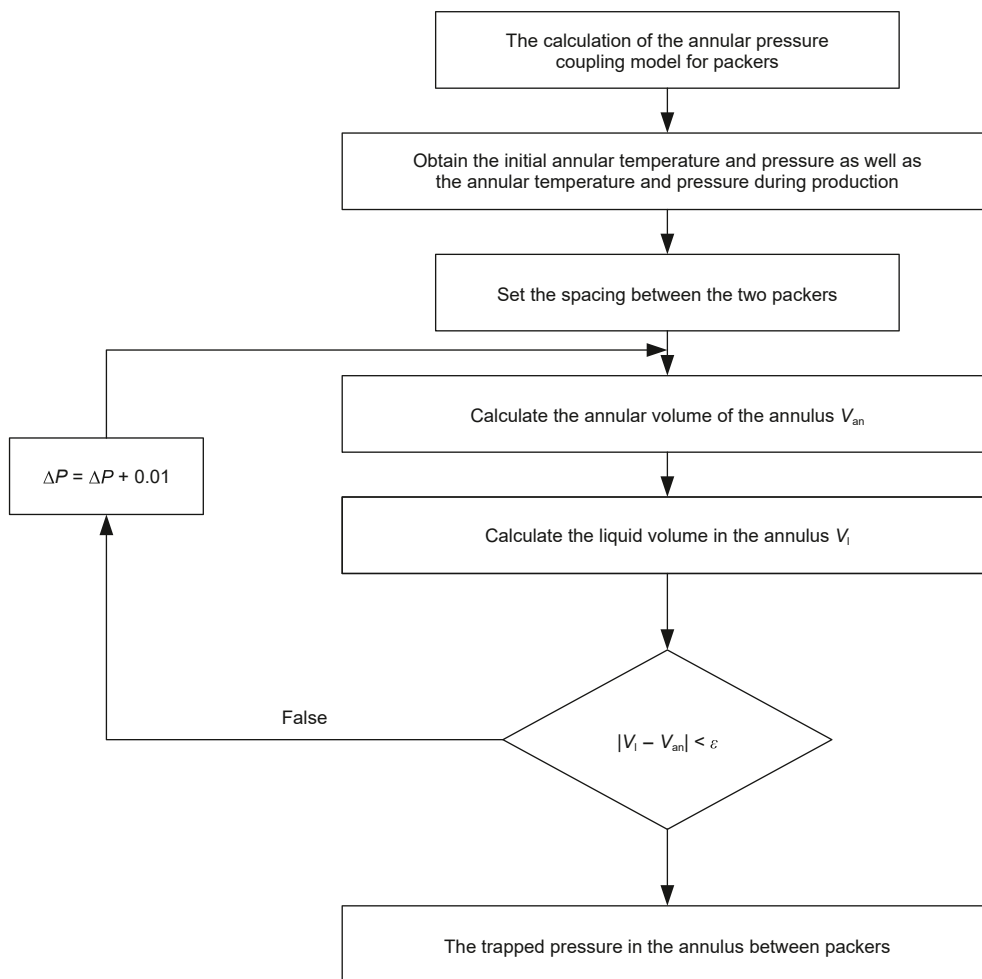


Fig. 8. Flow chart for calculation of annular pressure between packers.

Table 1
Experimental device and initial parameters.

Device	Size, mm	Initial parameters	A annulus	B annulus	C annulus
Tubing	88.9	Uncemented temperature, °C	62	51	43
Production casing	139.7	Uncemented well pressure, MPa	0.507	0.338	0.201
Technical casing	244.4	Cementing temperature, °C	65	54	42
Surface casing	339.7	Cementing pressure, MPa	0.694	0.275	0.404

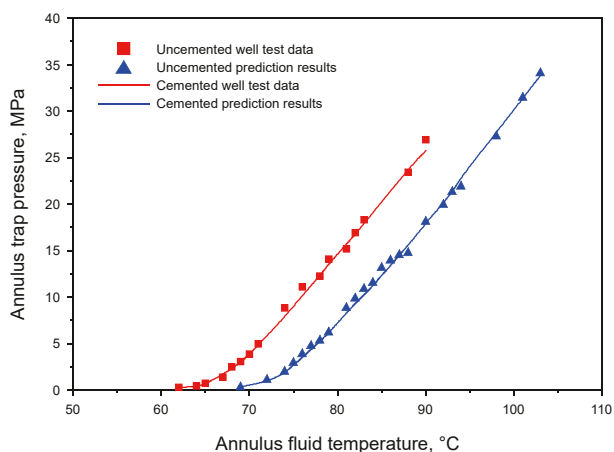


Fig. 9. Comparison of calculation data of APB model and experimental results in A annulus.

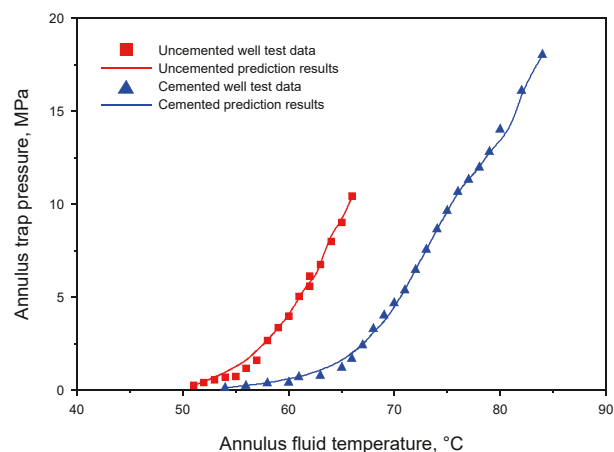


Fig. 10. Comparison of calculation data and experimental results of APB model in B annulus.

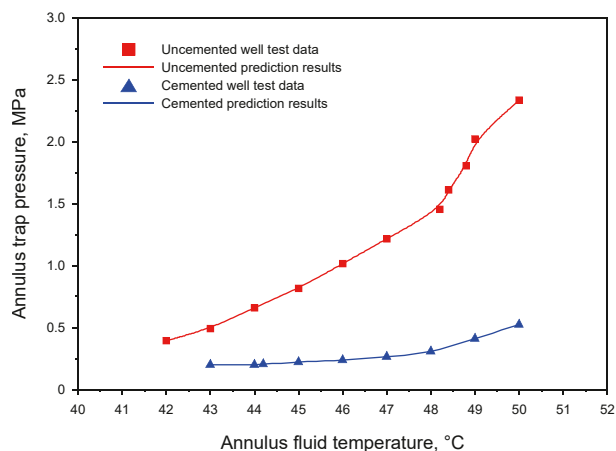


Fig. 11. C annular APB model calculation data and comparison of experimental results.

Table 2

Experimental and prediction error analysis results.

Condition	Annulus	Average error, MPa	RMSE	MAPE
Cementing	A	0.043	0.062	0.049
	B	0.102	0.150	0.123
	C	0.015	0.018	0.019
No cementing	A	0.129	0.190	0.167
	B	0.138	0.191	0.155
	C	0.008	0.009	0.010

with the experimental data, verifying the accuracy and effectiveness of the prediction model.

6. Conclusion

- (1) The mechanism of annular trap pressure increase is analyzed, and a multi-annular trap pressure prediction model was established based on the compatibility principle. It is proved that the model has high accuracy.
- (2) Based on the multi-annulus trap pressure prediction model, the case of nitrogen injection in annulus A was considered, and a gas-liquid two-phase multi-annulus trap pressure coupling model was established based on the BWSR state equation.
- (3) Based on the multi-annulus trap pressure prediction model, the annulus between double packers is considered, and a trap pressure prediction model for the annulus between double packers was established.

CRedit authorship contribution statement

Bo-Yuan Yang: Writing – original draft. **Hui Zhang:** Writing – review & editing. **Bao-Kang Wu:** Data curation. **Kun-Hong Lv:** Data curation. **Rui Yuan:** Methodology. **Yu-Ting Zhou:** Conceptualization. **Xing-Yu Li:** Writing – review & editing. **Ze Yang:** Methodology.

Conflict of interest

The authors declare that they have no conflicts of interest. None of the authors has any financial or non-financial interests, such as stocks, patents, consultancies, or grants, that could potentially

influence the objectivity, interpretation, or presentation of the research results in this paper. The research was conducted independently, and all data were collected, analyzed, and reported without any external bias.

Acknowledgements

This research was supported by the National Natural Science Foundation of China (Grant No. 52574017), National Major Science and Technology Project (Project No. 2025ZD1401905).

References

- Adams, A.J., Maceachran, A., 1994. Impact on casing design of thermal expansion of fluids in confined annuli. *SPE Drill. Complet.* 9 (3), 210–216. <https://doi.org/10.2118/21911-PA>.
- Deng, Y., Chen, P., Zhang, H., 2006. Iterative method for calculating the sealed annular pressure in oil and gas Wells. *Offshore Oil* 26 (2), 4. <https://doi.org/10.3969/j.issn.1008-2336.2006.02.019> (in Chinese).
- Dou, Y., Xue, S., Cao, Y., 2016. Coupling analysis of multi-annular pressure volumes in high-temperature and high-pressure well casings. *Petrol. Mach.* 44 (1), 71–74. <https://doi.org/10.16082/j.cnki.issn.1001-4578.2016.01.016> (in Chinese).
- Gao, B., 2002. Practical calculation model for casing loads induced by high temperatures. *Petrol. Drill. Prod. Technol.* 24 (1), 3. <https://doi.org/10.13639/j.odpt.2002.01.004> (in Chinese).
- Halal, A.S., Mitchell, R.F., 1994. Casing design for trapped annular pressure buildup. *SPE Drill. Complet.* 9 (2), 107–114. <https://doi.org/10.2118/25694-PA>.
- Jing, Y.H., Wang, T.B., Zhang, B., et al., 2025. Safety risk analysis of well control for wellbore with sustained annular pressure and prospects for technological development. *Chem. Technol. Fuels Oils* 61 (1), 110–119. <https://doi.org/10.1007/s10553-025-01844-9>.
- Liu, J.C., Fan, H.H., Peng, Q., et al., 2015. Research on the prediction model of annular pressure buildup in subsea Wells. *J. Nat. Gas Sci. Eng.* 27, 1677–1683. <https://doi.org/10.1016/j.jngse.2015.10.028>.
- Oudeman, P., Bacarreza, L.J., 1995. Field trial results of annular pressure behavior in a high-pressure/high-temperature well. *SPE Drill. Complet.* 10 (2), 84–88. <https://doi.org/10.2118/26738-PA>.
- Oudeman, P., Kerem, M., 2006. Transient behavior of annular pressure build-up in HP/HT wells. *SPE Drill. Complet.* 21 (4), 234–241. <https://doi.org/10.2118/88735-PA>.
- Sun, T.F., Zhang, X.Q., Wang, M.Z., et al., 2020. Experimental determination of drilling fluid thermal parameters when calculating APB. *Chem. Technol. Fuels Oils* 56, 87–95. <https://doi.org/10.1007/s10553-020-01114-w>.
- Sun, T.F., Han, Y.L., Yan, T.J., et al., 2024a. Study on the impact of weaving patterns of vibrating screen mesh on the performance of fluid flow through moving screens. *Geoenery Sci. Eng.* 234, 212643. <https://doi.org/10.1016/j.geoen.2024.212643>.
- Sun, T.F., Liu, Z.Y., Zhang, Y., 2024b. Rock breaking mechanism of saddle PDC cutters and analysis of mixed cutter layouts. *Rock Mech. Rock Eng.* 57 (11), 9903–9921. <https://doi.org/10.1007/s00603-024-04072-5>.
- Wang, H., 2023. Study on Casing Integrity of Horizontal Wells in Offshore Heavy Oil Thermal Recovery. Doctoral dissertation. China University of Petroleum (Beijing) (in Chinese).
- Wu, X.T., Wang, J.S., Feng, W., 2018. Study on annular trap pressure in deepwater oil and gas wells. *Petrol. Mach.* 46 (12), 47–50. <https://doi.org/10.16082/j.cnki.issn.1001-4578.2018.12.009> (in Chinese).
- Xu, F.H., 2019. Study on the Prediction and Prevention Measures for Sealing Pressure in Deepwater Test Wells. Master's Thesis. Yangtze University (in Chinese).
- Yang, J., Tang, H.X., Liu, Z.L., et al., 2013. Prediction model of casing annular pressure for deepwater well drilling and completion operation. *Petrol. Explor. Dev.* 40 (5), 661–664. [https://doi.org/10.1016/S1876-3804\(13\)60088-9](https://doi.org/10.1016/S1876-3804(13)60088-9).
- Yin, F., Gao, D., 2014. Improved calculation of multiple Annuli pressure buildup in Subsea HPHT Wells. In: IADC/SPE Asia Pacific Drilling Technology Conference. <https://doi.org/10.2118/170553-MS>.
- Zhang, B., Guan, Z.C., Zhang, Q., 2015a. Prediction of sustained annular pressure and the pressure control measures for high pressure gas wells. *Petrol. Explor. Dev.* 42 (4), 567–572. [https://doi.org/10.1016/S1876-3804\(15\)30051-3](https://doi.org/10.1016/S1876-3804(15)30051-3).
- Zhang, B., Guan, Z.C., Zhang, Q., 2015b. Prediction and analysis on annular pressure of deepwater well in the production stage. *Acta Pet. Sin.* 36 (8), 1012–1017. <https://doi.org/10.7623/syxb201508013>.
- Zhang, B., Guan, Z.C., Sheng, Y.A., et al., 2016. Impact of wellbore fluid properties on trapped annular pressure in deepwater wells. *Petrol. Explor. Dev.* 43 (5), 869–875. [https://doi.org/10.1016/S1876-3804\(16\)30104-5](https://doi.org/10.1016/S1876-3804(16)30104-5).
- Zhang, B., Guan, Z.C., Lu, N., et al., 2018. Current status and prospects of research on sealed annular pressure regulation technology in oil and gas wells. *China*

- Offshore Oil Gas 30 (6), 135–144. <https://doi.org/10.11935/j.issn.1673-1506.2018.06.017> (in Chinese).
- Zhang, L.L., Wang, P., Zhang, H., et al., 2021. Research on the calculation model of annular pressure between dual packers. *Petrol. Mach.* 49 (2), 104–109. <https://doi.org/10.16082/j.cnki.issn.1001-4578.2021.02.016> (in Chinese).
- Zhang, X., 2017. *Mechanical Analysis of Production Tubing in Heavy Oil Thermal Recovery Horizontal Wells*. Master's Thesis. China University of Petroleum, Beijing (in Chinese).
- Zhang, Y., Han, Y., Wu, B., et al., 2024a. Study on the flow characteristics of Non-Newtonian drilling fluid through vibrating screen meshes. *SPE J.* 1–11. <https://doi.org/10.2118/223632-PA>.
- Zhang, Y., Han, Y., Wu, B., et al., 2017. Study on the flow characteristics of Non-Newtonian drilling fluid through vibrating screen meshes. *SPE J.* pp. 1–11. <https://doi.org/10.2118/223632-PA>.
- Zhang, Y., Li, Y.A., Kong, X.W., et al., 2024b. Temperature prediction model in multiphase flow considering phase transition in the drilling operations. *Pet. Sci.* 21 (3), 1969–1979. <https://doi.org/10.1016/j.petsci.2024.01.004>.
- Zhang, Y., Li, Y., Kong, X.W., et al., 2024c. Numerical study of gas invasion law in fractured reservoirs. *Phys. Fluids* 36 (2), 026605. <https://doi.org/10.1063/5.0189020>.
- Zhang, Z., Wang, H., 2017. Considering annular thermal expansion pressure analysis, high-temperature and high-pressure gas wellhead lift. *J. Eng. Thermophys.* 38 (2), 267–276. [cnki:sun:gcrb.0.2017-02-008](https://doi.org/10.1063/5.0189020) (in Chinese).